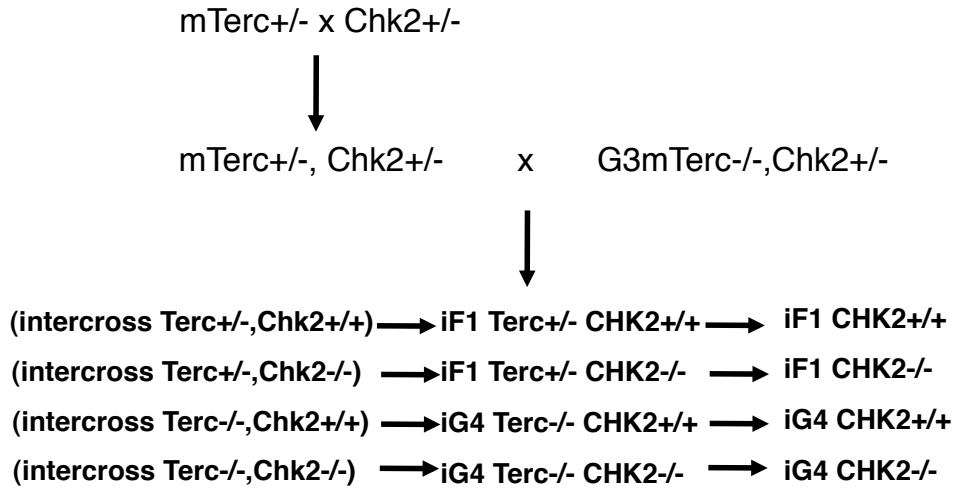
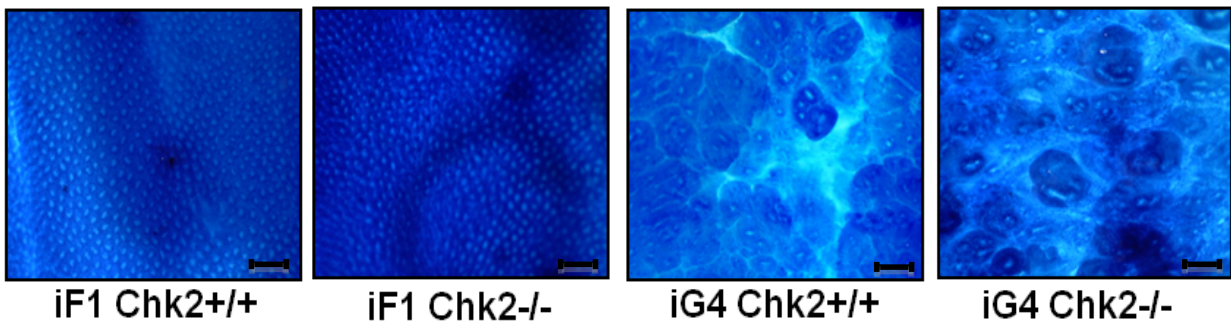


# Supplementary Fig\_1

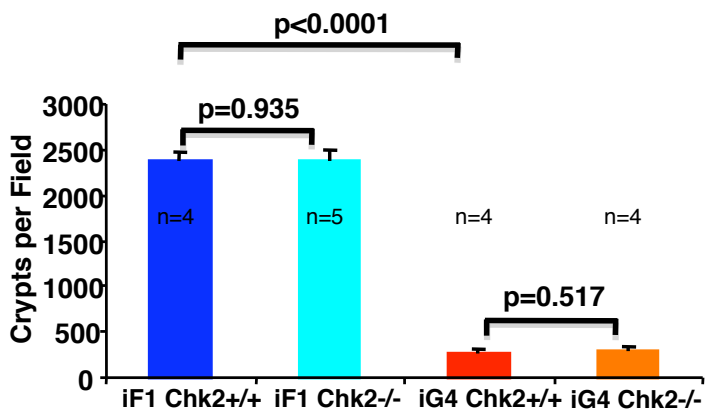
## A Mating Scheme



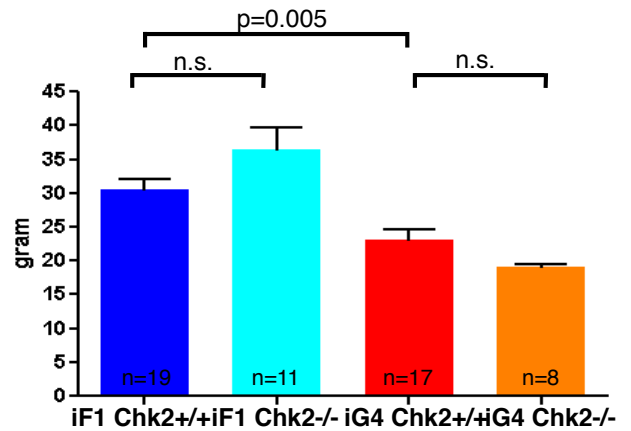
## B



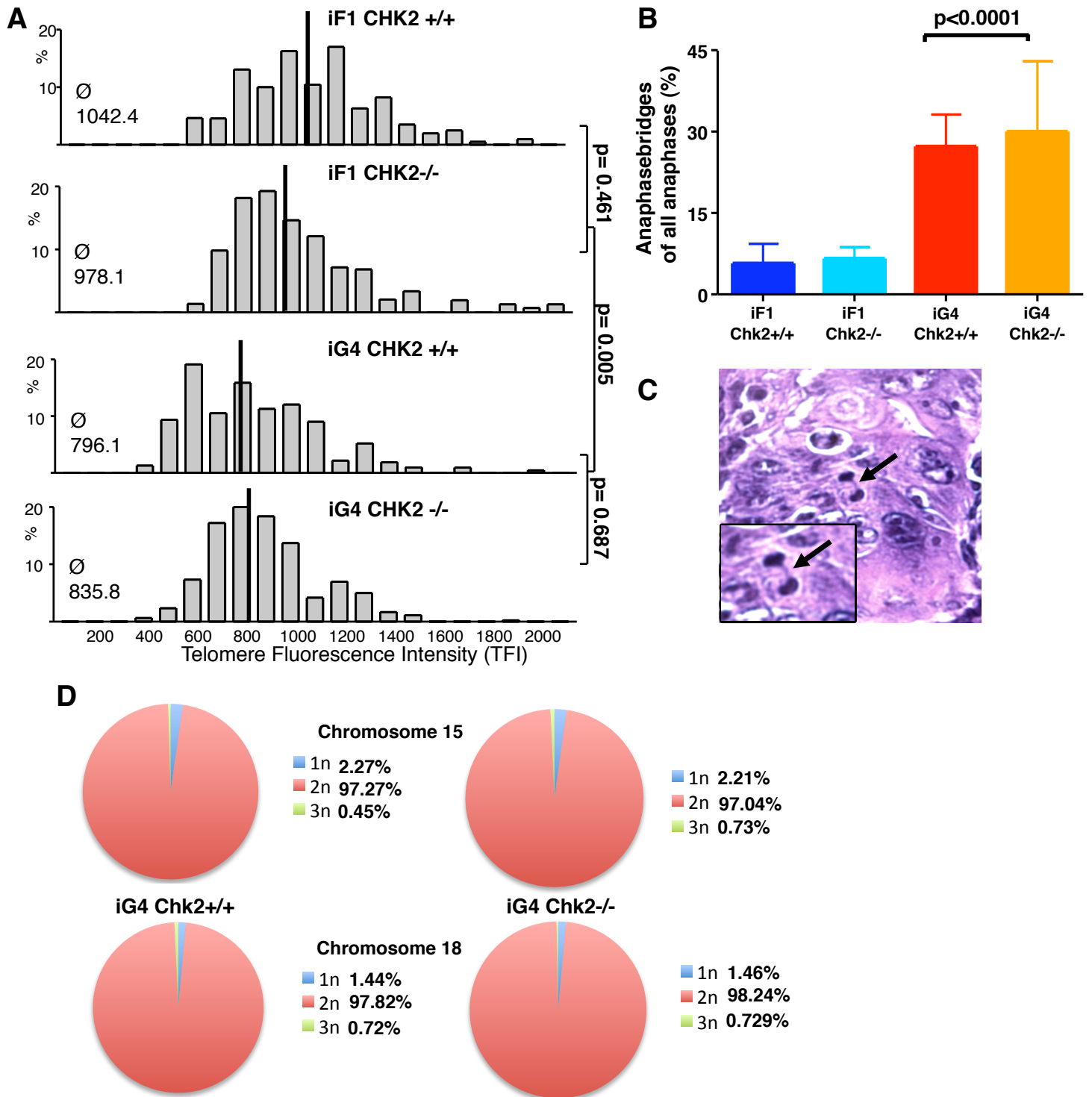
## C



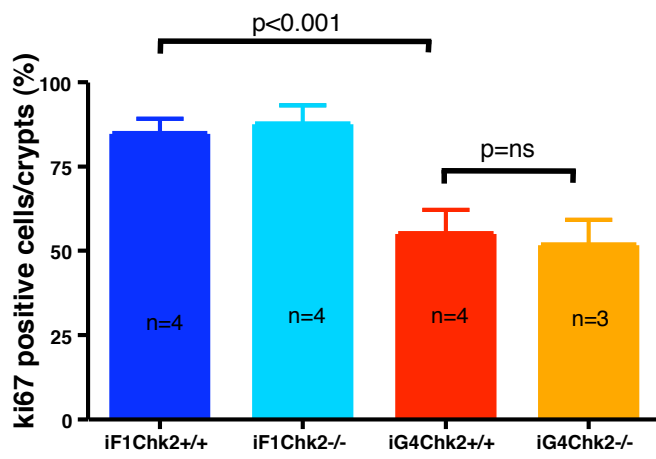
## D



## Supplementary Fig\_2

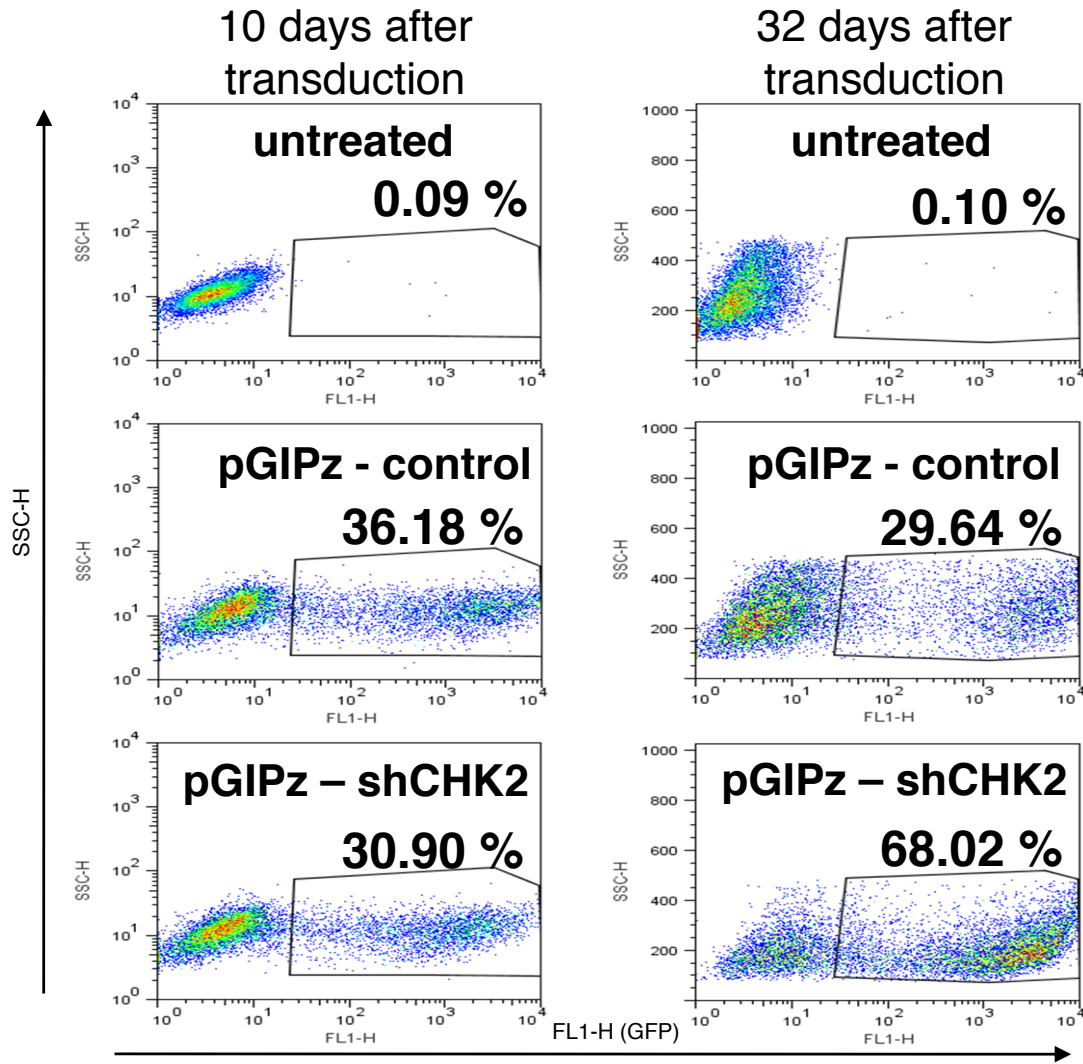


## Supplementary Fig\_3

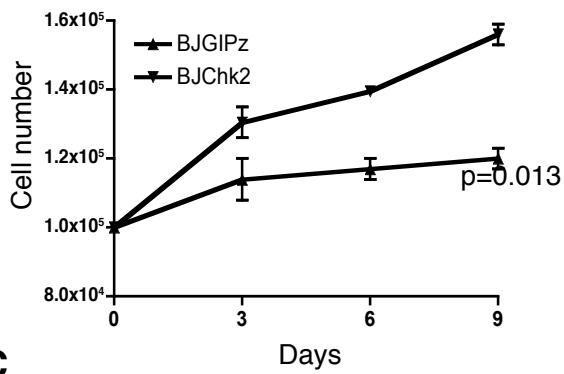


# Supplementary Fig\_4

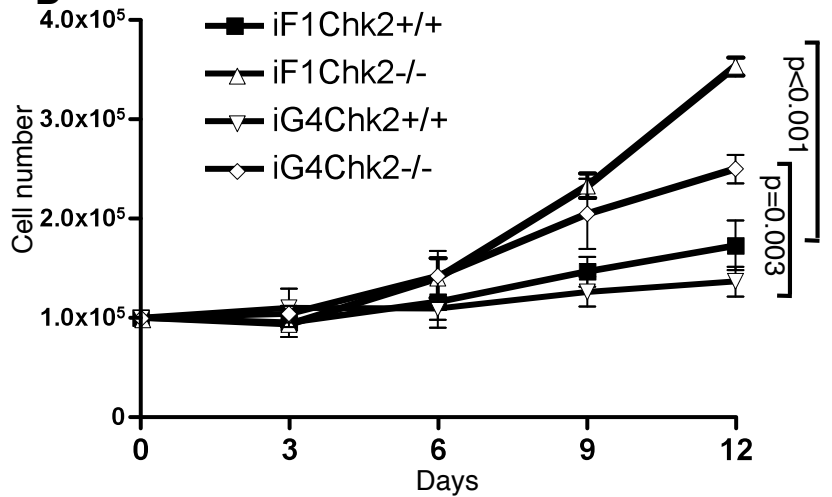
**A**



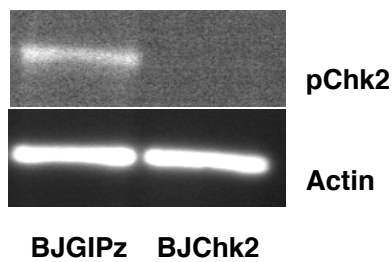
**B**



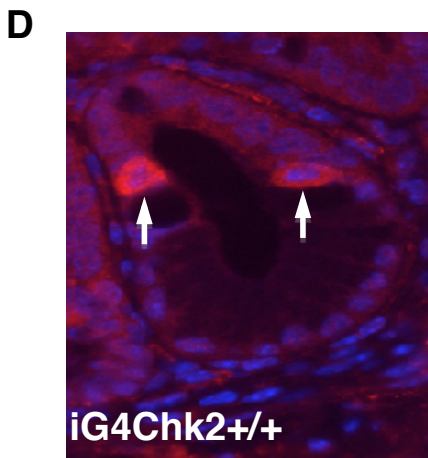
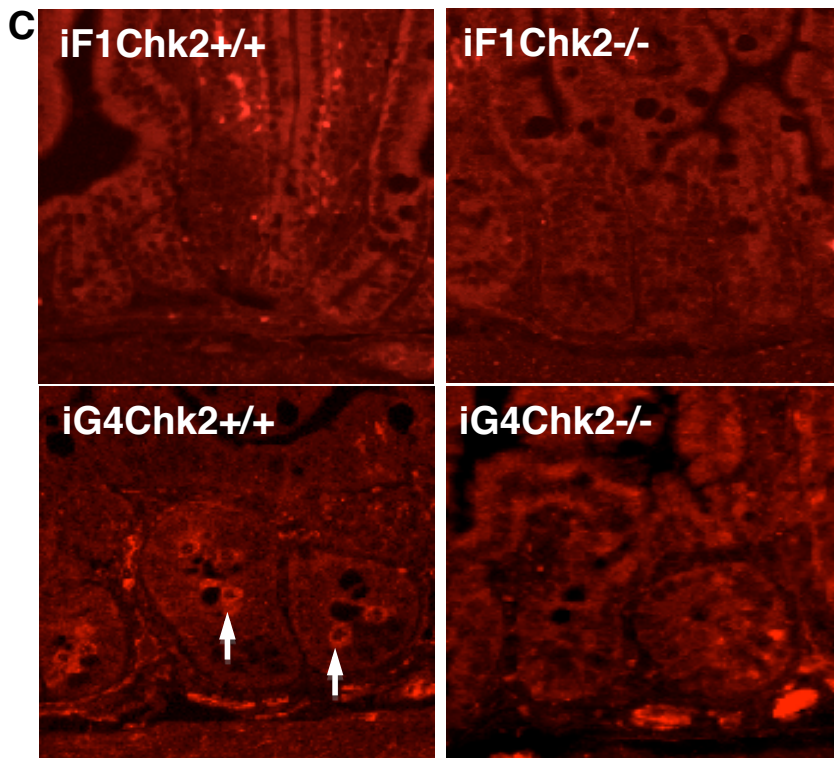
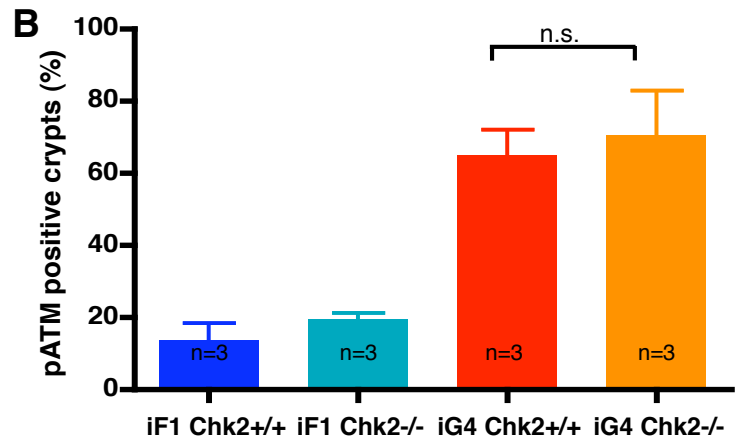
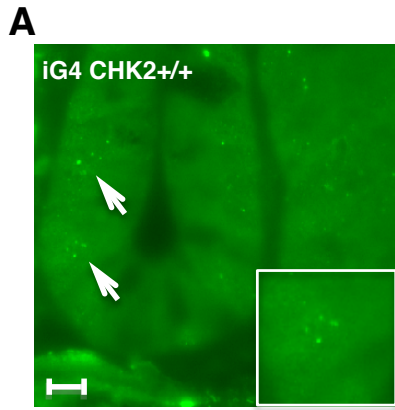
**D**



**C**

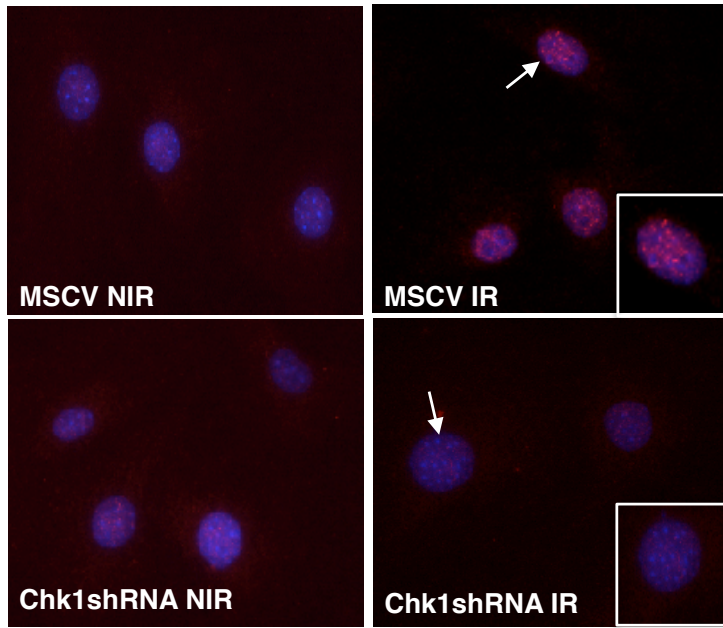


# Supplementary Fig\_5

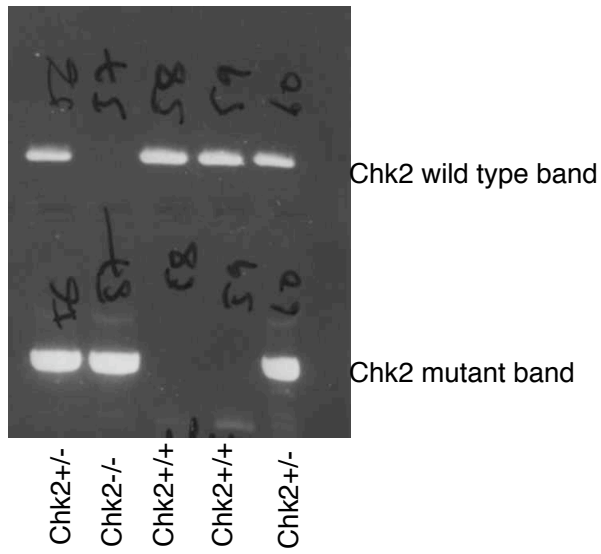


# Supplementary Fig\_6

**A**



**B**



## Supplementary Information

### Supplementary Figure legends

**Supplementary Figure 1.** (A) Mating scheme followed to produce experimental cohorts. mTerc<sup>+/-</sup>, Chk2<sup>+/-</sup> were mated with third generation G3 Terc<sup>-/-</sup>, Chk2<sup>+/-</sup> to produce the indicated, experimental cohorts. (B). Representative photographs of whole-mount staining of the colon of 9 to 12 month old mice of the indicated genotypes (magnification bar 500  $\mu$ m). (C) Histogram of the number of crypts per low-power vision field (35x) in the colon of 9 to 12 month old mice of the indicated genotypes (n = 4–5 mice per group; data are shown as mean; error bars represent standard deviation SD). (D) Histogram showing body weights of 9-12 month old mice of the indicated genotypes. (Data are shown as mean; error bars represent standard deviation SD).

**Supplementary Figure 2** (A) Telomere lengths in basal intestinal crypts of 9-12 month old mice. The diagram presents the distribution of the mean telomere fluorescence intensity (TFI) of individual crypts of mice of the indicated genotype (n=5 mice/group, n=30 crypts/mouse). The black line marks the mean TFI. iG4 Terc<sup>-/-</sup> mice exhibited shorter telomeres compared to iF1 Terc<sup>+/-</sup> mice (p=0.005), but Chk2 gene status had no significant effect on telomere length. (B) Histogram of the rate of anaphase bridges per total number of anaphases in basal crypts of small intestine of 9 to 12 month-old mice of the indicated genotypes (n = 5 mice per group; data are shown as mean; error bars represent SD). (C) Representative photographs showing an anaphase bridge in basal crypts of small intestine (magnification bar, 20  $\mu$ m). (D) Histograms showing the percentage of chromosome losses and gains of chromosome 15 and chromosome 18 of the indicated genotypes in the small intestine of the indicated genotypes.

**Supplementary Figure 3.** Histogram showing the percentage of ki67 positive cells per crypts in the small intestine of 9 to 12 month old mice of the indicated genotypes.

**Supplementary Figure 4.** (A) Representative FACS plots showing increase in the percentage of GFP positive BJ cells infected with CHK2 shRNA compared to empty vector control at different days after shRNA treatment. (B) Histogram of growth curves of BJ fibroblasts from empty vector control and CHK2 shRNA treated cells after sorting for GFP (p value refers to the data at day 9). (C) Western blot picture showing the knockdown of Chk2 in BJ fibroblasts. (D) Histogram of growth curve of mouse ear fibroblasts of the indicated genotypes (p values refer to the data at day 12) (Data are shown as mean; error bars represent SD at a given time point).

**Supplementary Figure 5.** (A) Representative photographs of phospho-ATM stained crypts in the small intestine of 9 to 12 month-old mice of the indicated genotypes (magnification bar, 600  $\mu$ m). (B) Histogram showing the percentage of phospho ATM positive crypts in the small intestine of 9 to 12 month old mice of the indicated genotypes (n = 3 mice per group; data are shown as mean; error bars represent SD). (C) Representative photographs of phospho-CHK2 staining in the small intestine of the indicated genotypes. Note that phospho CHK2 staining is only present in iG4 CHK2<sup>+/+</sup> mice. (D) Representative photograph of phosphoChk2 in the small intestinal crypt of a iG4Chk2<sup>+/+</sup> mouse. Nuclear counterstaining with DAPI indicates cytoplasmic localization of phospho-CHK2.

**Supplementary Figure 6.** (A) Immunocytochemistry for phospho Chk1 on primary mouse ear fibroblasts cells infected with a Chk1shRNA or empty vector (MSCV). Cells were irradiated 2 hrs before fixation with 6 Gy  $\gamma$ -irradiation or non-irradiated. Irradiation induced nuclear phospho-Chk1 staining is strongly diminished in shRNA-Chk1 infected cells. (B) Agarose Gel picture showing wild type band at 600bp and mutant band for Chk2 at 900bp. PCR primers are flanking Exons 8 - 11. In the wildtype mice a 600 base pairs fragment is amplified. In the Chk2 KO mouse Exons 8-11 are deleted. The PCR primers flanking Exon 8-11 result in a product of 900 base pairs. CHK2 knockout mice were kindly provided by Prof.Tak.W.Mak (Hirao et al, 2002).

## **Supplemental Methods**

### **Histopathological examination of tissues**

Mice were killed at the age of 9-12 months or at the time they appeared moribund. Various organs were retrieved and fixed in 4% formaldehyde over night before embedding in paraffin. Whole mounts of colon and rectum were prepared as previously described (Rudolph et al, 2001).

### **TUNEL Staining**

The rate of apoptosis was determined by TUNEL assay (In situ cell death detection kit, Roche, Mannheim, Germany) on 3  $\mu$ m thick paraffin sections of small intestine. The number of apoptotic cells per crypt was counted in 20 low-power fields (200x) per mouse (n = 4–5 mice per group).

### **Phospho CHK2 staining on fibroblasts**

(A) BJ fibroblasts were grown on coverslips and cells were fixed in 4% formaldehyde, permeabilized with 0.2% Triton X-100, washed twice with PBS, and then treated with phospho CHK2 antibody (1:200 dilution, Cell Signaling or Abcam) for 2 hrs. The secondary antibody (anti-rabbit Cy3-conjugated, Jackson laboratories) was used for 1 hr at room temperature. Phospho CHK2-foci-positive cells were counted in 40 low-power fields (400x).

### **FACS Analysis**

For flowcytometric analysis, hind limb bones were dissected and bone marrow single-cell suspensions were stained with antibody cocktails (BD Pharmingen) for 15 min on ice.

### **CHK2 shRNA experiments.**

The pGIPz-Vector\_containing CHK2-shRNA was purchased from Open Biosystems. 293T cells were transfected with shRNA construct and empty vector and viral

supernatant was collected at 24 hrs and 48 hrs after transfections and used to transduce late passage BJ fibroblasts. FACS analysis was performed for the cells, which are positive for GFP at 10 days and 32 days after transduction. Suppression of CHK2 was confirmed by western blotting.

### **Growth curves**

For shRNA treated BJ cells, GFP positive cells were sorted in both empty vector treated cells and CHK2-shRNA treated cells and  $1 \times 10^6$  cells were seeded in a cell culture dish and cells were trypsinised and counted using ViCell counter (Beckman). Mouse ear fibroblasts were isolated from mice and  $1 \times 10^6$  cells were seeded in a cell culture dish, cultured at 3% oxygen and cells were trypsinised and counted using ViCell counter (Beckman) at the indicated time points.

### **CHK1 shRNA**

Chk1shRNA against mouse is obtained from open biosystems in PSM2 vector backbone. This shRNA is sub cloned into MSCV retroviral backbone. Mouse ear fibroblasts were infected with retrovirus produced in phoamp cells. Both westernblot (data not shown) and ICC confirm knockdown of Chk1 in mouse ear fibroblasts.

### **Western Blot**

Whole-cell extracts of mouse ear fibroblasts or BJ fibroblasts or frozen small intestine of mouse were obtained in RIPA lysis buffer or NP-40 lysis buffer. Protein was subjected to 6 or 10% SDS-PAGE and detected using antibodies against phospho-Chk2 (T68) (1:1000, Cell Signaling), Phospho-CHK2(T68) (1:1000, Abcam), b-Actin (1:10000, Sigma) and Gapdh (1:10000, Bethyl laboratories), phospho ATM s1981 (1:1000, Cell signaling), ATM (1:1000, Abcam) phospho Chk1(1:1000, Cell signaling).

### **Q-Fish (Quantitative Fluorescence in Situ Hybridization)**

qFISH was performed as described (Rudolph et al, 2001; Satyanarayana et al, 2003) on 5  $\mu$ m thick paraffin sections of small intestine. Telomere length was analyzed from the nuclei of the basal crypts using the TFL-Telo Software from Peter Lansdorp.

**Chromosome FISH.** *In situ* FISH was performed as described (Begus-Nahrman et al, 2009) on 3  $\mu$ m thick paraffin sections of small intestine.

### **Chk2 Genotyping.**

PCR Primers:

WT1 - 5'-GTGTGCGCCACCACTATCCTG -3',

WT2 - 5'-CCCTTGGCCATGTTTCATCTG -3',

Mu1 - 5'- CAGGAGGTGGTGGCTTACTTTA -3'.

Mu2 - 5'- CAAATTAAGGGCCAGCTCATTC -3'.

For Chk2 wild type genotyping (1  $\mu$ g of DNA + 4  $\mu$ l 5X PCR buffer + 2  $\mu$ l 25mM MgCl<sub>2</sub> + 1.6  $\mu$ l dNTP's, 2.5mM each+ 1  $\mu$ l primer WT1(10 pmol) + 1.0  $\mu$ l WT2 (10 pmol) + 0.25  $\mu$ l Taq DNA polymerase + 8.15  $\mu$ l d.H<sub>2</sub>O). The PCR cycle profile is as follows: initial activation at 95°C for 1 min, 94°C for 15'', annealing at 58°C for 15'', and extension at 72°C for 1 min. Thirty cycles of PCR amplification were performed and the PCR products were run on 1.5% agarose gel and visualized with ethidium bromide (25  $\mu$ l of 1mg/ml conc. for 100ml of agarose gel). The primers amplify a fragment of 600 bp for Chk2 wild type mice.

For Chk2 Mutant genotyping (1  $\mu$ g of DNA + 5  $\mu$ l 5X PCR buffer + 1  $\mu$ l 25mM MgCl<sub>2</sub> + 2  $\mu$ l dNTP's, 2.5mM each+ 1  $\mu$ l primer Mu1(10 pmol) + 1.0  $\mu$ l Mu2 (10 pmol) + 0.5  $\mu$ l Taq DNA polymerase + 7.5  $\mu$ l d.H<sub>2</sub>O). The PCR cycle profile is as follows: initial activation at 95°C for 10', 94°C for 1', annealing at 60°C for 1', and extension at 72°C for 1 min. Forty cycles of PCR amplification were performed and the PCR products were run on 1.5% agarose gel and visualized with ethidium bromide (25  $\mu$ l of 1mg/ml conc. for 100ml of agarose gel). The primers amplify a fragment of 900 bp for Chk2 Mutant mice.

## References

Begus-Nahrman Y, Lechel A, Obenauf AC, Nalapareddy K, Peit E, Hoffmann E, Schlaudraff F, Liss B, Schirmacher P, Kestler H, Danenberg E, Barker N, Clevers H, Speicher MR, Rudolph KL (2009) p53 deletion impairs clearance of chromosomal-instable stem cells in aging telomere-dysfunctional mice. *Nat Genet*

Hirao A, Cheung A, Duncan G, Girard PM, Elia AJ, Wakeham A, Okada H, Sarkissian T, Wong JA, Sakai T, De Stanchina E, Bristow RG, Suda T, Lowe SW, Jeggo PA, Elledge SJ, Mak TW (2002) Chk2 is a tumor suppressor that regulates apoptosis in both an ataxia telangiectasia mutated (ATM)-dependent and an ATM-independent manner. *Mol Cell Biol* 22(18): 6521-6532

Rudolph KL, Millard M, Bosenberg MW, DePinho RA (2001) Telomere dysfunction and evolution of intestinal carcinoma in mice and humans. *Nat Genet* 28(2): 155-159

Satyanarayana A, Wiemann SU, Buer J, Lauber J, Dittmar KE, Wustefeld T, Blasco MA, Manns MP, Rudolph KL (2003) Telomere shortening impairs organ regeneration by inhibiting cell cycle re-entry of a subpopulation of cells. *EMBO J* 22(15): 4003-4013